

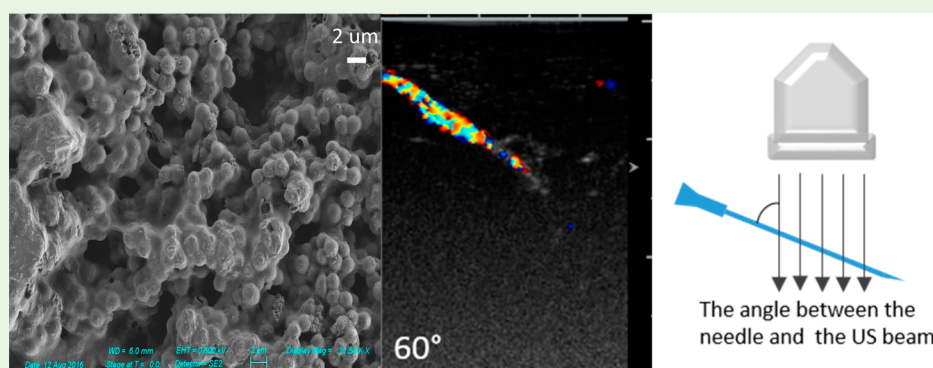
Silica Shells/Adhesive Composite Film for Color Doppler Ultrasound Guided Needle Placement

Jian Yang,^{*,†} Erin Ward,[‡] Tsai W. Sung,[§] James Wang,[§] Christopher Barback,^{||} Natalie Mendez,[⊥] Sarah Blair,[‡] William C. Trogler,[†] and Andrew C. Kummel[†]

[†]Department of Chemistry and Biochemistry, [§]Department of Nanoengineering, and [⊥]Materials Science and Engineering Program, University of California, San Diego, 9500 Gilman Drive, La Jolla, California 92093, United States

[‡]Department of Surgery, University of California, San Diego, 200 West Arbor Drive, San Diego, California 92103, United States

^{||}Department of Radiology, University of California, San Diego, 410 Dickinson Street, San Diego, California 92103, United States



ABSTRACT: Ultrasound (US) guided medical devices placement is a widely used clinical technology, yet many factors affect the visualization of these devices in the human body. In this research, an ultrasound-activated film was developed that can be coated on the surface of medical devices. The film contains 2 μm silica microshells and poly(methyl 2-cyanoacrylate) (PMCA) adhesive. The air sealed in the hollow space of the microshells acted as the US contrast agent. Ozone and perfluorooctyltriethoxysilane (PFO) were used to treat the surface of the film to enhance the US signals and provide durable antifouling properties for multiple passes through tissue, consistent with the dual oleophobic and hydrophobic nature of PFO. In vitro and in vivo tests showed that hypodermic needles and tumor marking wires coated with US activated film gave strong and persistent color Doppler signals. This technology can significantly improve the visibility of medical devices and the accuracy of US guided medical device placement.

KEYWORDS: silica shells, cyanoacrylate, film coating, ultrasound imaging, needle placement

INTRODUCTION

A variety of temporary and permanent implantable medical devices, such as needles, catheters, tumor biopsy markers, stents, and guidewires, are used clinically in human tissues. These devices are used for gaining central intravenous access, establishing regional nerve blocks, performing paracentesis, catheterization, tumor marking, and needle biopsies.^{1–5} Placement of medical devices requires a high accuracy and a wide margin of safety. Misplacement of those devices has the potential for serious consequences including nerve injury, hemorrhage, and false diagnostic results. Traditionally, an anatomic landmark technique is used to help the placement of medical devices.⁶ Successful placement of medical devices using an existing anatomic landmark is highly dependent on the operator's training and experience.⁷ Therefore, ultrasound (US) guided needle, catheter and guidewire placement has increasingly become the clinical standard. This technology uses real time visualization of both the anatomical structure and the approaching medical device to increase the efficiency and

accuracy of the operation and minimize the possibility of injury from misplacement.^{3,4,8–10}

Reflection of an ultrasound wave at an interface between two objects with different acoustic impedances produces ultrasonographic signals. Compared to soft tissues, metal or plastic medical devices have significantly different acoustic impedances which results in a strong ultrasound wave reflection between the devices and the tissue.¹¹ In ultrasound B-mode, the strength of the reflection is processed and displayed in grayscale. Metal or plastic objects in tissues are typically displayed with greater brightness relative to the soft tissue background which allows physicians to distinguish between the object and the surrounding soft tissue structures. In spite of the advantages of B-mode, US guided placement of medical devices is limited by poor visibility of medical devices in anatomically complex

Received: April 7, 2017

Accepted: June 6, 2017

Published: June 6, 2017

tissue structures. Each type of tissue has a different acoustic impedance and US can be reflected at the interfaces and generate complex echogenic signals that can make it difficult to differentiate between medical devices and the background. Close proximity to hyperechoic tissues such as fat and bone is especially challenging.¹²

Various strategies have been developed to improve the signal-to-noise ratio during US visualization of medical devices. Most of these methods focus on improving the visualization of needles used for biopsy or regional anesthesia. Roughening the surface of needles with an ampule file,¹³ coating the needles with a layer of polymer,^{14,15} or dimpling the surface of needles have all been reported to improve the needles' US visibility under B-mode.¹⁶ Tests of several commercial echogenic needles have been reported. Some mechanical or optical needle guides were developed to help the operator line up the US transducer and the needle in tissue. Perrella reported an US wave-activated piezoelectric polymer sensor fixed at the tip of a biopsy needle to produce a bright US signal.¹⁷ Su reported combining US and photoacoustic imaging methods to visualize a metal needle in tissue, but the technology requires a complicated pulsed laser system to produce a thermoacoustic response.¹⁸ In spite of these improvements, the greatest influence on the utility for B mode US imaging of medical devices remains the operator's skill.¹⁰

Other technologies have been developed to improve the accuracy of ultrasound guided implantation of medical devices by capitalizing on the unique attributes of an alternative ultrasound mode. Color Doppler ultrasound is a mode that is widely used within clinics for visualization and quantification of blood flow within the body. Doppler techniques can also be used to locate a moving object against a stationary background. The ColorMark device enables real time display of color Doppler signals by introducing vibratory motion in a needle.^{19,20} Manually moving the needle or adding a moving part in the needle can also produce a color Doppler signal.^{21,22} Currently, all the technologies that rely on color Doppler ultrasound require a moving object to produce a Doppler echo, which may sacrifice safety and efficiency. Moreover, attaching a moving part to the needle increases the cost, and the manual method of creating color Doppler signals required added complicated training for the medical professional.

It was reported previously that perfluorocarbon (PFC)-filled hard silica shells can be activated by clinical ultrasound equipment to produce color Doppler signals.²³ Ultrasound waves fracture the hard silica shells, which result in gas leakage and a decorrelation between two consecutive US pulses. This phenomenon can be observed with color Doppler imaging.²⁴ The long duration of US signals in tissues of PFB filled silica shells allows the shells to be used as a tumor marker.^{25,26} In another study, it was reported that medical devices coated in a 2 μm silica microshells/PMCA composite film can be located within the body cavity due to their ultrasound properties.²⁷ A macrophase separation during curing of the polymeric adhesive drives the microshells to the surface of the film and air is trapped in the hollow space by the hydrophobic polymer coating. The entrained air (instead of PFC) serves as the contrast agent under color Doppler US imaging.

The present report describes the use of 2 μm boron doped silica microshells/PMCA composite coatings on hypodermic needles and tumor marking wires to guide injection and marking with the aid of color Doppler US equipment commonly found within clinics. A new surface perfluorooctyl

coating was also employed to improve the persistence of US signals in animal tissues. The perfluorooctyl layer coated onto the surface of the film is both oleophobic and hydrophobic. This prevents fat sticking to the needles and water penetration into the film. In vitro and in vivo US properties of the coating were studied.

■ MATERIALS AND EXPERIMENTS

Materials. Two micrometer boron-doped silica microshells were synthesized following the previous report.²⁷ Loctite 430 super bonder instant adhesive (methyl 2-cyanoacrylate), which is designed for bonding to metal surfaces, was purchased from Henkel Corporation (Rocky Hill, CT). Perfluorooctyltriethoxysilane was purchased from Sigma-Aldrich. The 11/2" (3.8 cm) 21 gauge hypodermic needles were purchased from BD Medical (Franklin Lakes, NJ). The average thickness of the needle shaft was measured with use of a micrometer as $823 \pm 1 \mu\text{m}$ ($n = 4$). Tumor marking wire was purchased from Jorgensen Laboratories Inc. (Loveland, CO).

Fabrication of Silica Particles Containing PMCA Film. Ten mg of 2 μm silica microshells were suspended in 1.0 mL of DCM before 0.5 mL of methyl-2-cyanoacrylate adhesive was added. The glue/DCM/microshells mixture was coated on hypodermic needles and tumor marking wires by dipping the needles and wires into the liquid mixture for 4 cycles and the interval between each dipping was 2 min. The adhesive film was cured in air at room temperature for 24 h. The film thickness was measured with the use of a micrometer.

Ozone Processing of the Microshells/PMCA Film. Cured and coated hypodermic needles were exposed to ozone gas for 15 min. The flow rate of oxygen for ozone generation was set as 2L/min. The ozone gas was generated by the UVO Cleaner Model 42 (Jetlight Company, Inc.) with UV-light.

Modification of the Surface of Microshells/PMCA with Perfluorooctyltriethoxysilane. Ozone-processed and unprocessed hypodermic needles were dipped into 10 mL of 1% (v/v) perfluorooctyltriethoxysilane in methanol for 1 h before washing with ethanol and drying at room temperature in air overnight.

Electronic Microscopic Imaging and Contact Angle Measurements. Scanning electron microscopy (SEM) images of microshells and films were obtained using an FEI/Philips XL30 FEG ESEM microscope with an accelerating voltage of 1.5 kV. SEM samples were prepared by depositing coated needles on a carbon tape substrate. Combined field emission SEM (FE-SEM) images were obtained using a Sigma 500 FE-SEM (Zeiss, Germany) with an accelerating voltage ranging from 0.8 kV to 20 kV. FE-SEM samples were prepared with the same procedure employed for the SEM samples. The contact angles of the films were measured by analyzing the photograph of a water drop on the films with an ImageJ plugin from the NIH.²⁸

In Vitro and in Vivo Ultrasound Testing. In vitro and in vivo US tests were performed using a Siemens Acuson Sequoia 512 Ultrasound machine with the Acuson 15L8 transducer with a center frequency of 7 MHz. The software programs used for analysis of data include SanteDicom Viewer (Athens, Greece), ImageJ (National Institutes of Health, MA) and Microsoft Excel (Redmond, WA). Tests of ultrasound responsive film coated needles were performed in a water tank. The 15L8 US transducer was clamped in the water tank with the needle facing the transducer. The film was imaged with color Doppler ultrasound at a mechanical index (MI) of 1.9, which is the highest MI permitted by the FDA for diagnostic ultrasound imaging. The needles were kept in water and subjected to continuous ultrasound radiation for 60 min. The color Doppler signals were recorded over several time periods. The attenuating rates of color Doppler signals were studied by measuring the areas of the signals and comparing the areas with that of the initial signals using a MATLAB program (Mathworks, Natick, MA).

In vitro ultrasound testing of microshells/PMCA film coated needles was performed with a $6 \times 6 \times 3$ cm pork liver slice. A microshells/PMCA film coated needle was inserted into the tissue sample with different angles ranging from 0 to 45°. The distance between the needle tip and the surface of tissue sample was varied

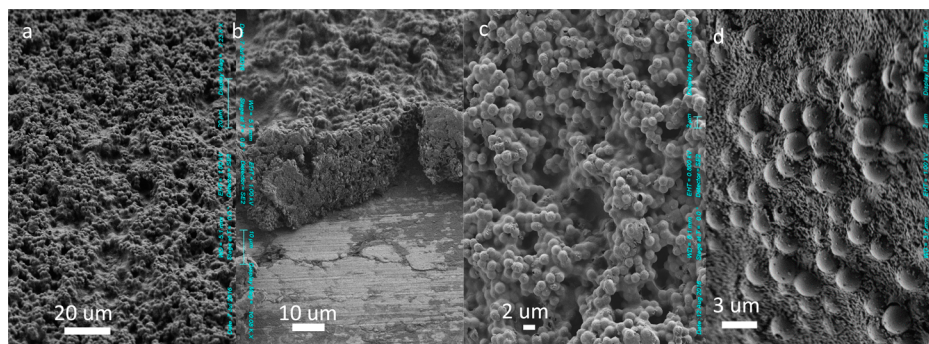


Figure 1. FE-SEM images of microshells/PMCA film (a) surface and (b) cross-section of and (c) ozone-processed and (d) ozone/PFO-processed microshells/PMCA films that were coated on hypodermic needles.

between 0.5 to 3 cm. Ultrasound properties were characterized with the use of an ACUSON Sequoia ultrasound system and a 15L8 transducer.

In vivo US testing of microshells/PMCA film coated needles and tumor marking wires was performed using female New Zealand white rabbits purchased from Western Oregon Rabbitry and housed individually in a UCSD vivarium facility. They were kept on a 12 h light/dark cycle and given water and Harlan Teklad commercial pellet diet ad libitum. All animal protocols were approved by the UCSD Institutional Animal Care and Use Program (IACUC).

Rabbits were anesthetized with isoflurane and placed on a circulating warm water pad. The abdomen was shaved and depilated. Gel was placed on the tip of the ultrasound transducer. Once anesthetized, the heart rate and SpO₂ of the rabbit were monitored via pulse oximetry. Furthermore, jaw tone, mucous membrane color, and pedal reflexes were also observed. Needles were inserted in the lower abdomen and imaged throughout. The surgeon used a 15L8 transducer to image the needle during introduction, maneuvering, and removal of needle so that ultrasound signals could be recorded. Tumor marking wire was inserted into the soft tissue and imaged with a 15L8 transducer.

RESULTS AND DISCUSSION

Synthesis of 2 μm Boron-Doped Silica Microshells and the Coating of Microshells/PMCA Films on Needles. The

Table 1. Thicknesses of the Microshells/PCMA Films on Surgical Needles before and after Surface Processing^a

film	unprocessed film	ozone processed film	PFO processed film	ozone and PFO processed film
thickness (μm)	34 ± 8	32 ± 10	34 ± 7	31 ± 8

^aThe thicknesses were measured with a micrometer, for four determinations.

2 μm boron -doped silica microshells were synthesized by the method reported previously.²⁷ Briefly, 2 μm polystyrene beads were used as the templates and the sol gel reaction²⁹ was employed to form silica shells on the templates before removing the polymer cores by calcining the core-shell particles at 550 $^{\circ}\text{C}$. The microshells exhibit a uniform nanoporous silica wall with a thickness of about 40 nm. Methyl 2-cyanoacrylate adhesive was used to bind 2 μm boron-doped silica microshells to the metal surface of needles. The microshells were dispersed in dichloromethane (DCM) before being mixed with the adhesive in order to ensure mixing and decrease the viscosity of the adhesive during coating.

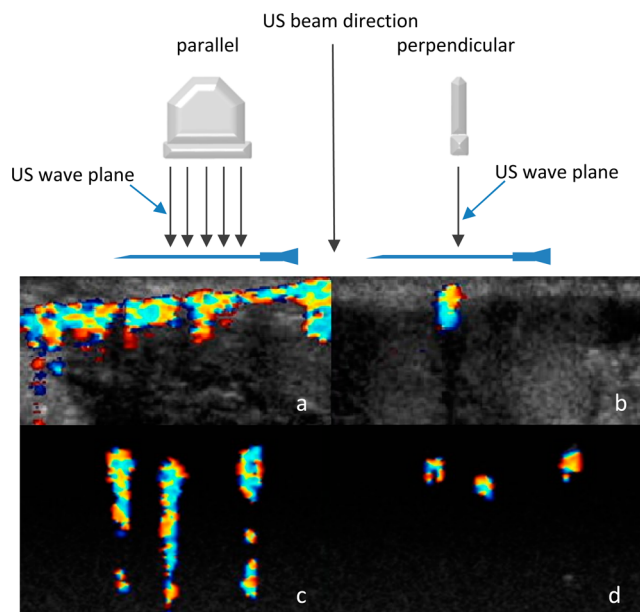


Figure 2. Silica microshells/PMCA film coated hypodermic needles were placed in a water tank with (a) parallel and (b) perpendicular positions to the US wave plane and color Doppler US images are shown for three microshells/PMCA film coated hypodermic needles in the water tank (c) before and (d) after 1 h of continuous insonation (all perpendicular to the US wave plane). Signals were obtained by a 15L8 transducer with a frequency of 7 MHz. Top schemes show the relative position of the needles, US wave plane and US beam direction.

Microshells/PMCA films were coated on needles or wires by dipping the needles and wires multiple times into the microshells/cyanoacrylate/DCM mixture. In previous research, it was found that increasing the number of dip coating cycles could increase the thickness of the film. In this research, the 11/2 in. 21G hypodermic needles were dipped into the coating agent four times. The average thicknesses of the microshells/PMCA film on the hypodermic needles was measured as $34 \pm 8 \mu\text{m}$ ($n = 4$).

It was reported previously that during the curing process, a macrophase segregation occurs and the microshells are driven to the surface of the film.²⁷ Figure 1a displays the STEM image of the microshells/PMCA film surface on a hypodermic needle. A loosely cross-linked microshells layer was observed. Figure 1b is the SEM image of the cross-section of microshells/PMCA film on a hypodermic needle, which shows a domain of polymer and microshells below the needle surface and a cross-linked microshell-enriched layer on the outer surface.

Attenuation Rate

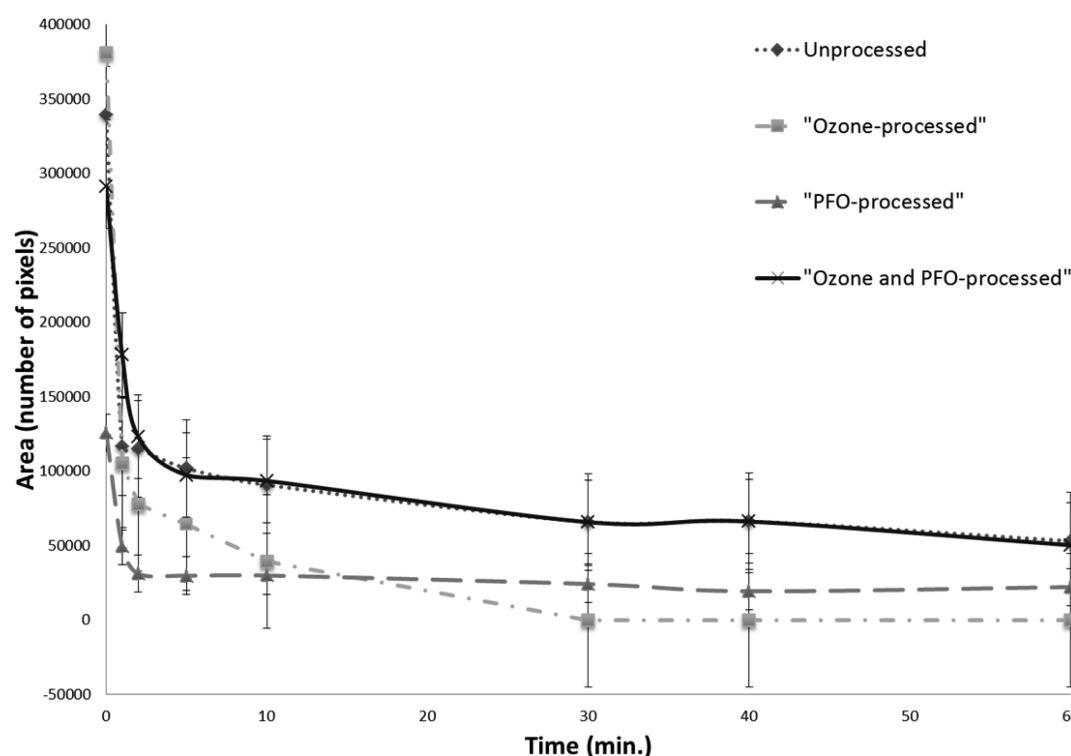


Figure 3. Attenuating rates of unprocessed and processed films on hypodermic needles during continuous insonation. The areas (number of pixels) of color Doppler signals were measured to represent the density of signals. Signals were obtained using a 15L8 transducer with frequency of 7 MHz.

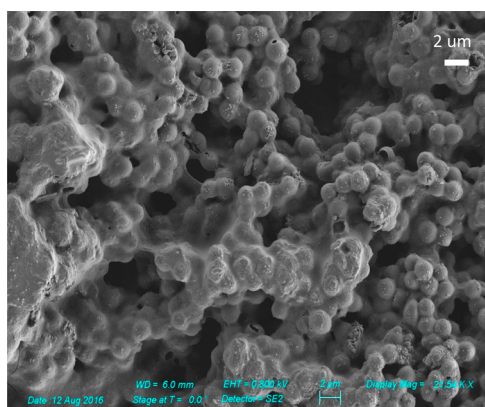


Figure 4. SEM image of microshells/PMCA film on a hypodermic needle after 3 h of continuous insonation.

Ozone Treatment and Surface Modification with Perfluorooctyl Groups. The microshells on the surface of film were thinly covered by polycyanoacrylate, which is hydrophobic. To improve the resistance of the film surface to adhering particles of tissues and fat during injection, ozone and a chemical treatment of the film surface were employed. Ozone can oxidize the surface of the polymer and produce reactive surface hydroxyl groups. After ozone treatment, the film was immediately coated with a nonstick layer of perfluorooctyl groups by dipping the film into a methanol solution of PFO for 1 h. The hydrophobicity of the surface before and after modification can be evaluated by measuring the contact angle of the film on a glass slide. Before ozone treatment, the average contact angle of the film was 70° , indicating that a hydrophobic

thin film of PMCA covers the silica microshells. After ozone treatment the average contact angle was 12° , which indicates that a large amount of hydroxyl groups were created by ozone-oxidization and turned the surface of the film from being hydrophobic to being hydrophilic. When the ozone-treated film was dipped in the methanol solution of PFO, the surface hydroxyls reacted with alkoxy silane to form Si–O bonds and grafted a layer of perfluorooctyl groups on the film surface. The average contact angle of the perfluorooctyl coated film with water was 68° . We also measured the contact angle of the hydrophobic solvent, octadecene to characterize the oleophobicity of the surface of the microshells/PMCA film. The contact angle of octadecene on the nontreated microshells/PMCA film and PFO modified microshells/PMCA film is 9 and 32° , respectively. Therefore, the current study reveals that the perfluorooctyl coating on the surface of the film is both oleophobic and hydrophobic, which simultaneously prevents fat from sticking to the needles, which causes damping of the US signal, and protects the film from water penetration, which displaces entrained air causing loss of the US signal. Figure 1c, d is the SEM images of the surface of an ozone-treated film and the surface of a perfluorooctyl modified film, respectively. No obvious change was observed after the ozone treatment and perfluorooctyl modification compared to the nontreated film, which implies that the ozone treatment and the grafting of perfluorooctyl group have only a superficial effect on the coating. The thickness of the film was measured after the ozone processing and PFO modification. Table 1 shows the thicknesses of the films were not significantly altered by either ozone treatment or the PFO groups.

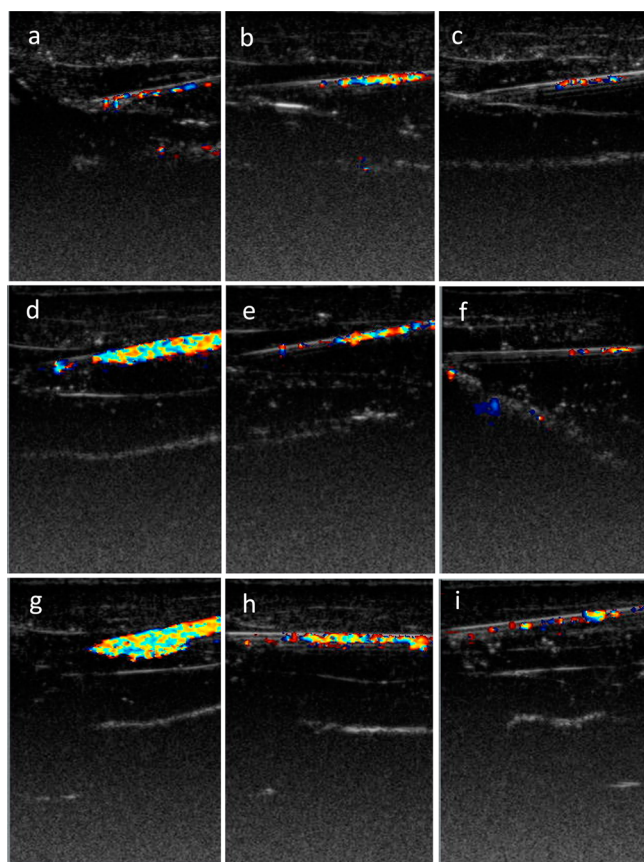


Figure 5. Color Doppler images of hypodermic needles with different surface treatment in pork liver. (a) Initial image of nonprocessed needle; (b) initial image of ozone processed needle; (c) image of ozone processed needle after 5 passes through the liver; (d) initial image of PFO coated needle; (e, f) images of PFO coated needle after 5 and 10 passes, respectively, through the liver; (g) initial image of ozone/PFO processed needle; (h, i) images of ozone/PFO processed needles after 15 and 20 passes, respectively, through the liver tissue.

In Vitro Ultrasound Studies. Figure 2a, b shows images of the color Doppler signals recorded for the microspheres/film coated needles in a water tank. Strong initial color Doppler signals were obtained from all needles in both the parallel (Figure 2a) and perpendicular positions (Figure 2b) with respect to the ultrasound wave plane. When the needle was imaged parallel to the ultrasound wave plane, the entire shaft of the needle could be visualized with color Doppler US. When the needle is perpendicular to the ultrasound wave plane, color Doppler signals of the needle cross section were seen as a

bright spot. The gas filled rigid silica shells can be fractured by ultrasound waves of high mechanical index (MI).³⁰ The gas released from ruptured silica shells causes local decorrelation events that can be imaged. In the microspheres/PMCA film, air was sealed in the hollow space of microspheres by the thin layer of hydrophobic polymer. When the microspheres were ruptured by the ultrasound wave, air escaped from the microspheres and expanded and contracted to produce the ultrasound image. As more microspheres are ruptured, the ultrasound signals become weaker because water replaces air in the hollow space of the microspheres. Figure 2c, d shows color Doppler signals of film-coated needles before and after 1 h of continuous insonation. The signals attenuated but did not disappear. The area of the signals of film-coated needles perpendicular to the ultrasound wave plane were measured versus time.

Figure 3 shows the attenuation rates of ultrasound signals of processed and unprocessed needles, respectively, on exposure to the continuous US wave. The density of ultrasound signals decreased quickly during the first 10 min. Since the transducer and needles were fixed in the water tank, there were approximately constant amounts of microspheres in the focal zone of the ultrasound waves. It is hypothesized that in the first 10 min, most of the microspheres in the ultrasound focal zone were ruptured. Then, a smaller subpopulation of microspheres with increasingly stronger walls, or deeper within the polymer film, was ruptured after 10 min and produced weaker ultrasound signals over the next 50 min. The ultrasound signals disappeared completely after 4 h. Figure 4 displays the SEM image of a film coated needle after 3 h of an ultrasound test. Compared to the initial SEM image (Figure 1) the microspheres appearance does not change significantly before and after the ultrasound test. This is probably because the thin polymer film coating the microspheres obscures tiny cracks or pits in the walls of the microspheres made by ultrasound cavitation at the surface.

Pork liver was used as a tissue phantom to study the ultrasound signals of the film coated needles. Figure 5 shows the color Doppler images of needles with different surface treatments embedded in pork liver. The signals from the nontreated needle were very weak (Figure 5a); after 5 passes through the liver tissues, the signals disappeared. When the needles were rinsed with ethanol after 5 passes through the tissues, ultrasound signals were recovered and comparable to the initial signal strength. It is hypothesized that some fat tissue or protein debris from the tissues packed tightly in the surface roughness of the film during the needle passing and dampened the ultrasound response.

After ozone processing, the initial signals of the needle were stronger than nontreated needles (Figure 5b) and this is consistent with weakening of the polymer film on the top layer

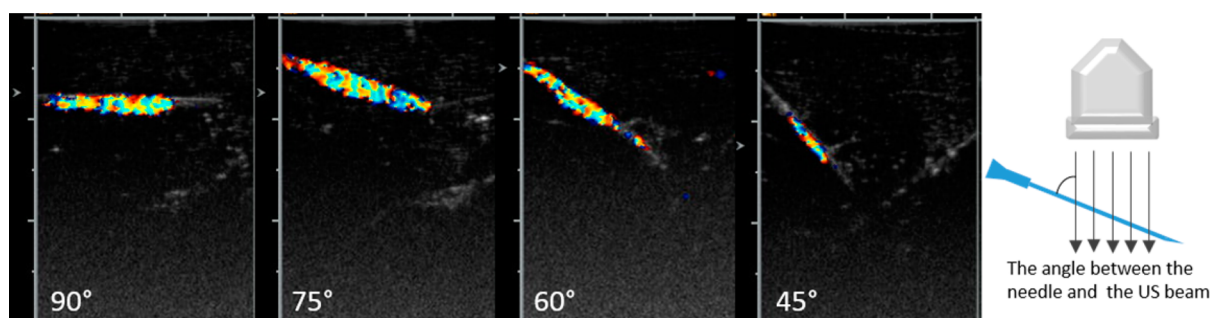


Figure 6. Color Doppler signals of ozone/PFO-treated hypodermic needles with different angles relative to US wave beam in pork liver.

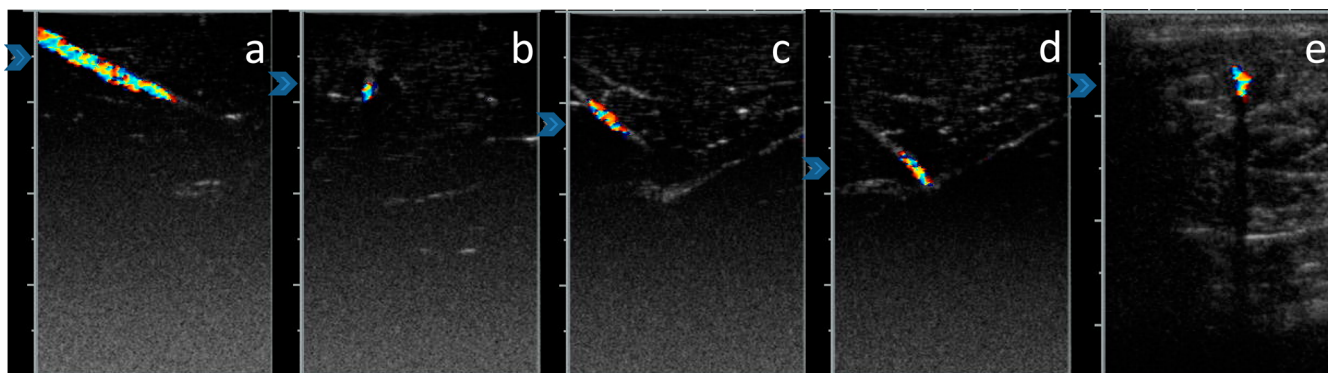


Figure 7. Color Doppler signals of (a–d) an ozone/PFO-processed hypodermic needle and (e) tumor marking wire in a live rabbit. In panel a, the needle is parallel with the US wave plane and the angle between the needle and the US beam is 30° . In panel b, the hypodermic needle is perpendicular to the US wave plane and the angle between the needle and the US beam is 30° . In panels c and d, the hypodermic needle is parallel with the US wave plane and US beam angle is 40° . In panel e, the wire is perpendicular to the US wave plane and the angle between the wire and the US beam is 30° .

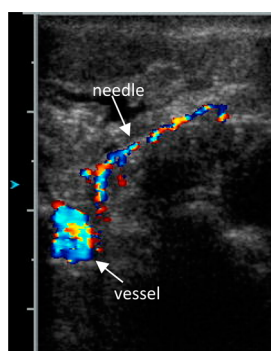


Figure 8. Color Doppler signals of an ozone/PFO-processed hypodermic needle and a blood vessel in a live rabbit.

of nanoshells by chemical reaction. However, the signals also diminished after 5 passes through the tissue (Figure 5c) and completely disappeared after 10 passes through the tissues. The ozone treatment produced a hydrophilic surface of the film, which is expected to lower the affinity of the hydrophobic polymer for the fat in the tissues, thereby allowing the signals to resist more passes. However, the opposite was observed. The data are consistent with a hydrophilic coating enabling water to enter the nanoshell/polymer film and quench the signal; however, it may be that more hydrophilic proteins adhere to the surface instead of fat. To increase the signal persistence after the ozone treatment, a surface modification is needed.

The needle surface modified with perfluorooctyl groups but without ozone pretreatment had stronger initial signals than ozone processed needles (Figure 5d); the signals were greatly enhanced compared to noncoated needles after 5 passes (Figure 5e) and abated after 10 passes through the tissue (Figure 5f). The data are consistent with dual oleophobic and hydrophobic properties being critical to a strong initial signal and a long signal persistence.

To achieve synergy between the ozone-treated polymer with more hydroxyls, we processed the PFO modification after ozone treatment. With this combination, the initial ultrasound signals of the needle were very strong (Figure 5g), and after 15 passes through the tissue, the signals remained strong (Figure 5h). The signals only became weak after 20 passes through the tissue (Figure 5i). The data are consistent with the ozone oxidation producing a high density of surface hydroxyl groups

which reacted with PFO to provide a more complete coating. In summary, the nonstick perfluorooctyl layer on the surface of the film is both oleophobic and hydrophobic, resulting in persistent ultrasound signals that were strong and could resist multiple passes of the hypodermic needle through the tissues.

The angle between the shaft of the needle and US beam has a significant effect on the needle visibility.^{11,16} The ozone/PFO-treated needles were used to test the color Doppler image quality in pork liver with various insertion angles relative to the US transducer plane. Figure 6 shows the images with different transducer alignment angles. When the angle ranges from 90° to 60° , the complete shaft of the needle is clearly observed. When the angle is larger than 60° , the focal pointer (the arrow at the left of the image) had to be adjusted to locate the tip or the shaft of the needle. For a 15L8 transducer on Sequoia 512 US system, the focal pointer moves the focal zone 0.25 cm toward or away from the transducer. Echoes outside the focal zone will not produce significant images, which is consistent with just imaging the end of the needle at small angles.

In Vivo Detection Study. Figure 7a displays the color Doppler image of an ozone/perfluorooctyl-treated needle in a live rabbit. The angle between the shaft and the US beam is 65° . Similar with the results in pork liver, at this angle the entire shaft of the needle was visible and the signals were strong. Figure 7b is the color Doppler image of the needle at same angle but the needle was perpendicular to the US wave plane. Figure 7c and d show color Doppler images of the needle in the live rabbit with an angle of 35° . At this angle, only a portion of the needle could be visualized. The arrow on the left of the image indicates the focal zone of the US imaging. Adjusting the focal zone made the central shaft (Figure 7c) or the tip (Figure 7d) of the needle visible, but the signals were not as strong as the signals of needles imaged with a larger angle.

Figure 8 shows the US signals of a coated hypodermic needle in the pelvis of a live rabbit. The needle was approaching a blood vessel. The vessel is about 2 cm from the surface of the skin but the US signals from the film allowed clear observation of the relative positions of the needle tip and the blood vessel. To image the entire needle, the needle had to be precisely parallel to the ultrasound waves. When the needle was perpendicular to the US wave plane, the needle was easily located by US imaging; however, the position of the needle tip was difficult to identify even with subtle changes in the transducer placement along the needle by the surgeon.

CONCLUSION

An ultrasound activated film containing 2 μm silica microshells and cyanoacrylate adhesive was used to cross-link and bind microshells on the surface of hypodermic needles and tumor marking wires. The air sealed in the hollow space of microshells acted as an US contrast agent after its release during insonation. In vitro and in vivo studies showed that the microshells/PMCA films imparted strong color Doppler signals using clinical US equipment. To improve the US image, ozone processing and then applying a PFO surface coating gave the microshells/PMCA film both oleophobic and hydrophobic chemical properties. This results in macroscopic antifouling properties during multiple needle passes in animal tissues. This technology demonstrates potential applications of such coatings to enable accurate placement of hypodermic needles for biopsy, intravenous access, and wire markers with the aid of US imaging.

AUTHOR INFORMATION

Corresponding Author

*E-mail: jy183@ucsd.edu.

ORCID

Jian Yang: [0000-0002-0106-1396](https://orcid.org/0000-0002-0106-1396)

William C. Trogler: [0000-0001-6098-7685](https://orcid.org/0000-0001-6098-7685)

Andrew C. Kummel: [0000-0001-8301-9855](https://orcid.org/0000-0001-8301-9855)

Notes

The authors declare the following competing financial interest(s): A.C.K. and W.C.T., scientific cofounders, have an equity interest in Nanocyte Medical, Inc., a company that may potentially benefit from the research results, and serve on the company's Scientific Advisory Board. S.L.B. has a family member with an equity interest in Nanocyte Medical, Inc., a company that may potentially benefit from the research results. The terms of this arrangement have been reviewed and approved by the University of California, San Diego, in accordance with its conflict of interest policies.

ACKNOWLEDGMENTS

Financial support was provided by a grant from RF Surgical System Inc, a subsidiary of Covidien-Medtronic Inc. The authors acknowledge the California Institute for Telecommunications and Information Technology for use of electronic microscopy facilities in the Nano3 cleanroom.

REFERENCES

- Hermans, J.; Bierma-Zeinstra, S. M.; Bos, P. K.; Verhaar, J. A.; Reijman, M. The most accurate approach for intra-articular needle placement in the knee joint: a systematic review. *Semin. Arthritis Rheum.* **2011**, *41*, 106–115.
- Sofocleous, C.; Schur, I.; Cooper, S.; Quintas, J.; Brody, L.; Shelin, R. Sonographically guided placement of peripherally inserted central venous catheters: review of 355 procedures. *AJR, Am. J. Roentgenol.* **1998**, *170* (6), 1613–1616.
- Chapman, G.; Johnson, D.; Bodenham, A. Visualisation of needle position using ultrasonography. *Anaesthesia* **2006**, *61* (2), 148–158.
- Stone, M. B.; Moon, C.; Sutijono, D.; Blaivas, M. Needle tip visualization during ultrasound-guided vascular access: short-axis vs long-axis approach. *Am. J. Emerg. Med.* **2010**, *28* (3), 343–347.
- Eloubeidi, M. A.; Chen, V. K.; Eltoum, I. A.; Jhala, D.; Chhieng, D. C.; Jhala, N.; Vickers, S. M.; Wilcox, C. M. Endoscopic ultrasound-guided fine needle aspiration biopsy of patients with suspected pancreatic cancer: diagnostic accuracy and acute and 30-day complications. *Am. J. Gastroenterol.* **2003**, *98* (12), 2663–2668.
- Hayashi, H.; Amano, M. Does ultrasound imaging before puncture facilitate internal jugular vein cannulation? Prospective randomized comparison with landmark-guided puncture in ventilated patients. *J. Cardiothorac. Vasc. Anesth.* **2002**, *16* (5), 572–575.
- Hannan, L.; Reader, A.; Nist, R.; Beck, M.; Meyers, W. J. The use of ultrasound for guiding needle placement for inferior alveolar nerve blocks. *Oral Surg. Oral Med. Oral Pathol.* **1999**, *87* (6), 658–665.
- Hopkins, R.; Bradley, M. In-vitro visualization of biopsy needles with ultrasound: a comparative study of standard and echogenic needles using an ultrasound phantom. *Clin. Radiol.* **2001**, *56* (6), 499–502.
- Williams, D.; Sahai, A.; Aabakken, L.; Penman, I.; Van Velse, A.; Webb, J.; Wilson, M.; Hoffman, B.; Hawes, R. Endoscopic ultrasound guided fine needle aspiration biopsy: a large single centre experience. *Gut* **1999**, *44* (5), 720–726.
- Schafhalter-Zoppoth, I.; McCulloch, C. E.; Gray, A. T. Ultrasound visibility of needles used for regional nerve block: an in vitro study. *Reg. Anesth. Pain Med.* **2004**, *29* (5), 480–488.
- Chin, K. J.; Perlas, A.; Chan, V. W.; Brull, R. Needle visualization in ultrasound-guided regional anesthesia: challenges and solutions. *Reg. Anesth. Pain Med.* **2008**, *33* (6), 532–544.
- Sites, B. D.; Chan, V. W.; Neal, J. M.; Weller, R.; Grau, T.; Koscielniak-Nielsen, Z. J.; Ivani, G. The American Society of Regional Anesthesia and Pain Medicine and the European Society of Regional Anaesthesia and Pain Therapy joint committee recommendations for education and training in ultrasound-guided regional anesthesia. *Reg. Anesth. Pain Med.* **2010**, *35* (2), S74–S80.
- Laine, H.; Rainio, J. An inexpensive method of improving visualisation of the needle tip in fine needle aspiration biopsy (FNAB). *Ann. Chir. Gynaecol.* **1993**, *82*, 43–45.
- Gottlieb, R. H.; Robinette, W.; Rubens, D.; Hartley, D.; Fultz, P.; Violante, M. Coating agent permits improved visualization of biopsy needles during sonography. *AJR, Am. J. Roentgenol.* **1998**, *171* (5), 1301–1302.
- Charboneau, J. W.; Reading, C. C.; Welch, T. J. CT and sonographically guided needle biopsy: current techniques and new innovations. *AJR, Am. J. Roentgenol.* **1990**, *154* (1), 1–10.
- Nichols, K.; Wright, L. B.; Spencer, T.; Culp, W. C. Changes in ultrasonographic echogenicity and visibility of needles with changes in angles of insonation. *J. Vasc. Interv. Radiol.* **2003**, *14* (12), 1553–1557.
- Perrella, R.; Kimme-Smith, C.; Tessler, F.; Ragavendra, N.; Grant, E. A new electronically enhanced biopsy system: value in improving needle-tip visibility during sonographically guided interventional procedures. *AJR, Am. J. Roentgenol.* **1992**, *158* (1), 195–198.
- Su, J.; Karpouk, A.; Wang, B.; Emelianov, S. Photoacoustic imaging of clinical metal needles in tissue. *J. Biomed. Opt.* **2010**, *15* (2), 021309–021309–6.
- Feld, R.; Needleman, L.; Goldberg, B. B. Use of needle-vibrating device and color Doppler imaging for sonographically guided invasive procedures. *AJR, Am. J. Roentgenol.* **1997**, *168* (1), 255–256.
- Armstrong, G.; Cardon, L.; Vilkomerson, D.; Lipson, D.; Wong, J.; Rodriguez, L. L.; Thomas, J. D.; Griffin, B. P. Localization of needle tip with color Doppler during pericardiocentesis: In vitro validation and initial clinical application. *J. Am. Soc. Echocardiogr.* **2001**, *14* (1), 29–37.
- Kurohiji, T.; Sigel, B.; Justin, J.; Machi, J. Motion marking in color Doppler ultrasound needle and catheter visualization. *J. Ultrasound Med.* **1990**, *9* (4), 243–245.
- Hamper, U. M.; Savader, B. L.; Sheth, S. Improved needle-tip visualization by color Doppler sonography. *AJR, Am. J. Roentgenol.* **1991**, *156* (2), 401–402.
- Martinez, H. P.; Kono, Y.; Blair, S. L.; Sandoval, S.; Wang-Rodriguez, J.; Mattrey, R. F.; Kummel, A. C.; Trogler, W. C. Hard shell gas-filled contrast enhancement particles for colour Doppler ultrasound imaging of tumors. *MedChemComm* **2010**, *1* (4), 266–270.
- Lieberman, A.; Martinez, H. P.; Ta, C. N.; Barback, C. V.; Mattrey, R. F.; Kono, Y.; Blair, S. L.; Trogler, W. C.; Kummel, A. C.; Wu, Z. Hollow silica and silica-boron nano/microparticles for contrast-

enhanced ultrasound to detect small tumors. *Biomaterials* **2012**, *33* (20), 5124–5129.

(25) Liberman, A.; Wang, J.; Lu, N.; Viveros, R. D.; Allen, C.; Mattrey, R.; Blair, S.; Trogler, W.; Kim, M.; Kummel, A. Mechanically Tunable Hollow Silica Ultrathin Nanoshells for Ultrasound Contrast Agents. *Adv. Funct. Mater.* **2015**, *25* (26), 4049–4057.

(26) Liberman, A.; Wu, Z.; Barback, C. V.; Viveros, R.; Blair, S. L.; Ellies, L. G.; Vera, D. R.; Mattrey, R. F.; Kummel, A. C.; Trogler, W. C. Color doppler ultrasound and gamma imaging of intratumorally injected 500 nm iron–silica nanoshells. *ACS Nano* **2013**, *7* (7), 6367–6377.

(27) Yang, J.; Wang, J.; Ta, C. N.; Ward, E. P.; Barback, C. V.; Sung, T.-W.; Mendez, N.; Blair, S. L.; Kummel, A. C.; Trogler, W. C. Ultrasound Responsive Macrophase Segregated Microcomposite Films for In Vivo Biosensing. *ACS Appl. Mater. Interfaces* **2017**, *9* (2), 1719–1727.

(28) Pegoretti, A.; Dorigato, A.; Brugnara, M.; Penati, A. Contact angle measurements as a tool to investigate the filler–matrix interactions in polyurethane–clay nanocomposites from blocked prepolymer. *Eur. Polym. J.* **2008**, *44* (6), 1662–1672.

(29) Liberman, A.; Mendez, N.; Trogler, W. C.; Kummel, A. C. Synthesis and surface functionalization of silica nanoparticles for nanomedicine. *Surf. Sci. Rep.* **2014**, *69* (2), 132–158.

(30) Ta, C. N.; Liberman, A.; Martinez, H. P.; Barback, C. V.; Mattrey, R. F.; Blair, S. L.; Trogler, W. C.; Kummel, A. C.; Wu, Z. Integrated processing of contrast pulse sequencing ultrasound imaging for enhanced active contrast of hollow gas filled silica nanoshells and microshells. *J. Vac. Sci. Technol., B: Nanotechnol. Microelectron.: Mater., Process., Meas., Phenom.* **2012**, *30* (2), 02C104.